Patch Based Deep Local Feature Learning and Self Similarity Multi Level Clustering for Neonatal Brain Segmentation in MR Images

Puja Shashi, Suchithra R

Abstract: ***The main purpose of this work is to develop a new scheme to profoundly retrieving features to perform the process of identifying a brain regions from the MR neonatal brain image. First the input MR neonatal brain image is denoised by using the Modified Fuzzy Adaptive Non Local Mean Filter (FANLMF) and then the contrast of the image is enhanced using the Adaptive Average Intensity Based Histogram Equalization (AAIHE). After pre-processing the input MR image, the next step is to retrieve the features of a similar image. To capture the features from the pre-processed image, this project offers a new technique for retrieving features called Patch Based Deep Local Feature Learning (PBDLFL). After retrieving the deep features, the next step is to divide the brain regions based on these retrieved features. To implement this process, the supervised segmentation scheme is employed. Among several supervised segmentation scheme this works employs proposed approach named Self Similarity Multi Level Clustering (SSMLC). Finally, the retrieved features are given as an input to these SSMLC approach for separating the regions of the brain. To understand the effectiveness of the proposed deep feature retrieval and proposed segmentation scheme, four performance metrics are employed namely, Dice Similarity Coefficient (DSC), Positive Predictive Value (PPV), Jaccard Index (JI) and Sensitivity (SEN). The experimental results show that the new PBDLFL and SSMLC perform better than other existing approaches.***

Keywords : Neonatal Brain, AAIHE, FANLMF, MDBUTMF , PBDLFL and SSMLC

I. INTRODUCTION

Specific distribution of fetal brain images of white matter (WM), gray matter (GM), and cerebrospinal fluid (CSF) in the first year of life is crucial in the study of early brain development. Recognizing specific brain abnormalities immediately after birth enables us to predict autism. For this purpose, magnetic resonance imaging (MRI) is a preferred model for mimicking a newborn's brain, as it is safe, invasive, and provides multiple transverse brain segments. However, segmenting the fetal brain on MRI is a difficult problem due to factors such as decreased tissue volume, increased noise, artifacts, movement, or continued diffusion of white matter in the fetus. To address this problem, several methods have been proposed [3]. Popular methods use several atoms to model the anatomic variability of brain tissue [16, 15]. However, the implementation of techniques that rely solely on atlas synthesis is limited. Expansion of labels or adaptation methods such as matrix models or deformation models [14] can be applied to improve preliminary estimates of tissue probabilities [14].

However, one of the major drawbacks of using such a method for fetal brain segmentation is the high risk of error due to differences in fetal size. In addition to getting the right segment, these methods usually require a lot of explanatory images, which takes time and requires a lot of experience. In recent years, in-depth training methods have been proposed as an effective alternative to the methods described above. In particular, Neural Networks (CNNs) have been successfully used to solve various problems with medical imaging, achieving the leading results in many applications [21, 13, 12, 26, 5] including brain tissue. Distribution of infants [25, 28, 6]. For example, [25] suggests a 2D CNN architecture large enough to obtain accurate and consistent segments from a single image. In order to overcome the problem of low tissue contrast between WM and GM, the work has considered many modalities as input to the CNN.

In [28], MR-T1, T2, and fractional anisotropy (FF) images were combined at the time of network integration. Similarly, Nie et al. [6] proposed a fully resolved neural network (FCNN) in which these model images were processed in three independent ways and the corresponding features were subsequently merged for final classification. However, these methods present some important limitations. First, some architectures [25,28] adopt a window scrolling strategy in which the region defined by the window is operated in the same region. This results in poor results and unstructured predictions that reduce the accuracy of the classification. Second, these methods often use 2D patches as input into the network, completely abandoning the anatomical context in the direction oriented to the 2D plane. As shown in [12], considering a three-dimensional collapse instead of 2D results in a better distribution. In view of the challenges and challenges mentioned above, we propose a new segmentation method called DCADC. The paper summary is as follows. Section 2 gives a short literary work. Section 3 gives a brief outline of the pre-process methodology, segmentation, and technique for retrieving features.

Manuscript published on November 30, 2019.
* Correspondence Author
Puja Shashi, Associate professor, HOD MSc IT, Jain University.
Suchithra R, Director of MCA department in Jain Deemed to be University,Bangalore

© The Authors. Published by Blue Eyes Intelligence Engineering and Sciences Publication (BEIESP). This is an open access article under the CC-BY-NC-ND license http://creativecommons.org/licenses/by-nc-nd/4.0/

This section also presents the complete technological scheme of the proposed work. Section 4 explains the set of data used to assess the performance and the indicators used for this assessment. Finally, the conclusion of this work is illustrated in Section 5.

II. BACKGROUND

Most of the newborn brain tissue distribution techniques rely on the layout of the brain. The popularity of taxi cards stems from their widespread utility. They guide the process of fragmentation in areas of weak contrast and help differentiate tissues with similar intensities. The Atlantic, which is aided by image distortion strategies, also helps to bring images of different themes together. Although there are many brain diagrams for adults [17], the price charts for children, especially for newborns and infants, are few. However, many authors prefer to make their brain diagrams from locally available NMR arrays using manual or semi-automated methods [30], [24]. This section provides an overview of the various layouts used and the strategies of their respective divisions.Mapping brain maps based solely on reference manuals takes a lot of effort and time. But handmade electronics are more reliable because they are closer to basic truths. It is also useful when the focus is on the different anatomical configurations of the brain. A classic case of Atlas-based classification is the case of Gousias et al. [8] Their Alberta atlas was constructed by manually separating the MR brain into 15 premature infants and newborns. There were 5 in 50 sites [9]. The ALBERTs created are in public domain 11 for use by other researchers. These sculptures were used in automated MR imaging of newborns by Gousias et al. [8] In two ways

Initially, several ALBERTs were used for label distribution, followed by voxel labeling, which was achieved by consensus decision based on Kittler et al. [20] The following method involves propagation of the label of maximum likelihood structure constructed for the newborn ALBERT (MPNA), which is similar to the maximum likelihood child graph used in Gousias et al. [7] The two methods were compared and the results were validated against the gold standard by hand. In a subsequent paper, Makropoulos et al. [1] proposed a modified EMM scheme that incorporates right brain models and levels of knowledge based on partial volume correction. An important aspect of the work is the improvement of its accuracy on previous studies (Gousias 2013) and the program regarding gestational age from 24 weeks to the approximate age.

The distribution of eight classes of adapters by Melbourne et al. [2] It is also based on prior knowledge gained from manual distribution. Brain and tissue masks were extracted from the manual annotated training dataset; They were distorted on object images using homology and deformity based on the Modat et al. [11] To achieve higher status. Subsequent tissue segmentation includes the macrocyclic macroscopic algorithm for surface smoothing, followed by partial volume correction used in Cardoso et al. [18] The features of the method are MWM extraction and separation of air ducts from the CSF. The work of Egekher et al. [19] also used the reference section as Atlas. But the difference is the use of the Atlantic for each object, based on the "let go" principle.This practice provides the necessary pre-allocation information without requiring very large databases. The use of multiple markers in combination with tag synthesis has provided a consistent map for each tissue. Each tissue map is combined with a controlled classification result based on the nearest K classifier (K-NN). Bayesian classifiers are used to resolve voxels with multiple or no tissue functions, and each tissue segment is combined. Another work that relies on extensive pre-manual classification is the work of Yu et al. [29] This method uses manual segmentation of sub-structures based on previously published work [23,22].

The manual annotation outlines nine structures: the brain, the brain, the brain, the amygdala, the hippocampus, the acoustics, the thalamus, the spleen, and the spleen. In addition, GM, WM and CSF semi-automatic allocation was performed. The classification is based on the 2d feature map extracted from the manual training data annotated and further enhanced by the hidden MRF-EM scheme. This is adapted from the unified approach Sajja et al. [4] which is intended for brain MRI in adults. Finally, manual tissue maps and semi-automatic results were incorporated. The use of manual annotations makes this method reliable but less reproducible than automated techniques.

Prastawa et al. [21] introduced a method of tissue segmentation based on an asymptotic approximation of core density. New developments in the work include dividing between the umbilical and non-vertebral classes according to graphical adhesion techniques (minimum branching) and removal of residues using least-squares scattering estimates. The epidermal tissue space is reproduced by a probabilistic probability. The disadvantage is that Atlas is made up of an average of half of the three subjects and therefore cannot cover a large disparity in neurological populations. In previous work [26], we introduced the EM scheme and introduced a similar Markov random field (MRF) scheme [28] to apply smoothing labels.

A novelty of this work is the introduction of a knowledge-based method that defines MPMs to adjust for the binding components of improperly labeled CSF voxels such as WM in the CGM-CSF interface. In addition, primary tissue-specific primers were evaluated by a clustering agent, eliminating the use of atoms for size examples. Xue et al. Only the CSF, CGM, and WM tissue sections hide the structure of the gray matter. Weisenfeld et al. [12] used the same model editing process to evaluate distributions using STAPLE [12]. Partial volume correction was performed by the method similar to [8] and the homogeneity of the model by MRF. The tissue distribution by Weisenfeld et al. It depends on the initial alignment of the bundles of matter, which is incredible because of the large differences in the brain development of newborns at different ages.

Other methods for segmenting the NMR brain include the use of graphs [6], where the word integral probability is estimated using non-symmetric density estimation techniques. In their work [6] Song et al. Extensive image processing has been approved. Song et al. Only the gray and white sections do not include the skull and CSF with the manual outline. Cardoso et al. [1] [2] proposed an EM-MRF scheme that adapts Assam similar to [13]. Atlas taken from the poster are modeled from the distribution of the dichotomous and adapted according to each imam's poster.

Sectional volumes were modeled using a multivariate distribution between different tissues.

In addition, Cardoso et al. Turning away from the classical Gaussian model, introducing half a Gaussian before the Gaussian mean tissue was started with a manually selected patch sample. Cardoso et al. Avoid relying on atlas alignment with a primary relaxation scheme. However, when splitting a structure with a similar intensity profile, it is unclear how the relaxation scheme would adapt the propagation, for example, in the structure of the gray matter. More detailed sections of a large number of brain regions are needed to evaluate changes in regional brain volume over time. Recently, one of the first methods was developed in [10] to show that T1-weighted MR images can be automatically and reliably distributed using multi-Atlantic methods.

In a atlas-based segmentation method, the MR image of a hand-held object is usually not rigorous to the MR image, and its label is propagated to it based on the computational calculations [14]. The distributed labels of the various icons can be combined to obtain the possible number of deviations or to give the final result of the distribution. One of the most commonly used techniques (by a majority vote) of labeling [3], [10], [14], [15], identifies each voxel with the most preferred Atlantic structure. More sophisticated synthesis techniques weigh the votes of each Atlas on the basis of the MR image of Atlas with the images subdivided [16] [17]. Labeling (by majority or regional vote) is among the most effective techniques when allocating multiple regions. [10] [17] [18]

To overcome the above limitations of previous brain tumor investigations on our mine detection systems, we offer a new approach based on hybrid features that include information from handy and deep training options. The objective of this work are.

1. To develop a proposed segmentation approach called Deep Collaborative Affinity Dictionary Clustering (DCADC).
2. To develop a segmentation approach (DCADC) even works well in closed contour objects.
3. To develop a non sensitive segmentation approach (DCADC) without asking any initialization parameters.
4. To achieve high segmentation accuracy than the other existing approaches..

In the next section, we proposed our method to segment neonatal brain segmentation from the MR image, which we reduced by overcoming the limitations found on this subject.

A. Submission of the paper

Author (s) can send paper in the given email address of the journal. There are two email address. It is compulsory to send paper in both email address.

III. MATERIALS AND METHODS

The overall architecture for the brain segmentation based supervised learning has been shown in Fig. 1. First the input MR brain image is denoised by using Fuzzy Adaptive Non Local Mean Filter (FANLMF) and then the image contrast is enhanced by using the Adaptive Average Intensity Based Histogram Equalization (AAIHE). After pre-processed the input image the next step is to retrieve the features from the denoised and contrast enhanced image. To retrieve the features from the pre-processed image this project proposed one proposed feature retrieval technique named Patch Based Deep Local Feature Learning (PBDLFL). After retrieving these deep features the next step is to partition the brain segmentation based on these retrieved features. To do this process the supervised segmentation scheme is employed. Among sever supervised segmentation scheme this works employs deep machine learning approaches named Deep Collaborative Affinity Dictionary. Finally the retrieved features are given as input to these machine learning approaches to partition the brain regions.

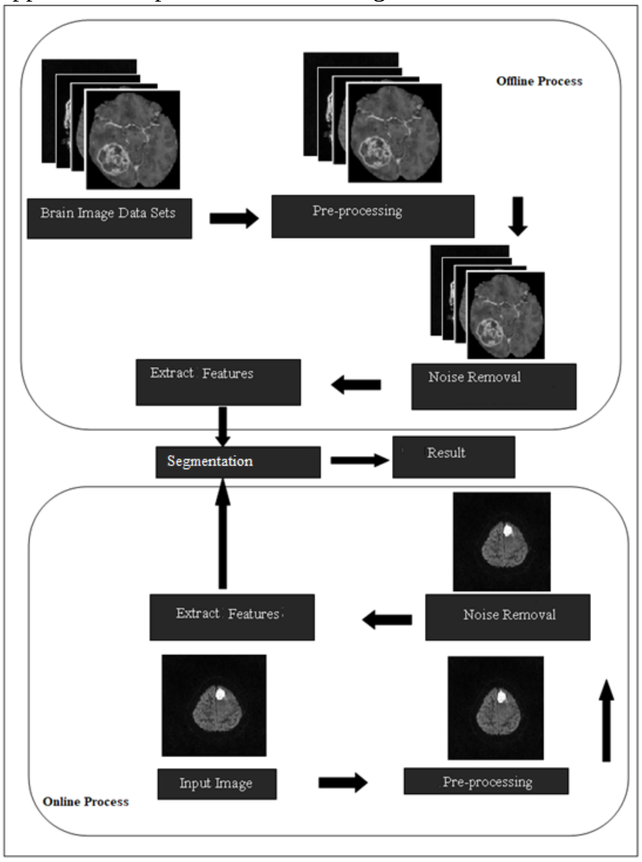

Fig 1. Overall Architecture of the Proposed Work

A. Pre-processing

First, for the primary infrared image of the MR brain is enhanced by adaptive techniques. Analogue alignment (AAIHE) is a computer image processing technology employed to increase image levels. It differs from the simple histogram alignment, because many histogram manipulation methods, each corresponding to a particular part of the image, use them to distribute the light of the image. So it is suitable for improving the local contrast and improving the edge definitions in each area of the image. However, AAIHE has a tendency to exaggerate noise in areas with the same image. The variant isotope variant called AAIHE, as opposed to the histogram, changes it by limiting the profit margin. Chip algorithms are shown in # 1 algorithm and the magnetization effect of nuclear magnetism using AAIHE is shown on the in Fig. 2.

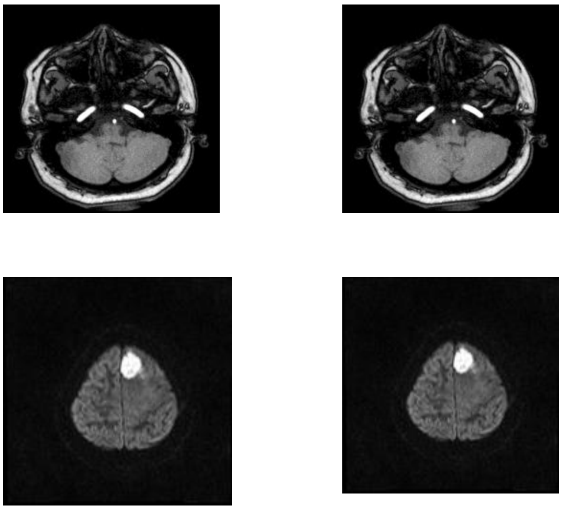

(a) (b)

Fig. 2(a). input MR Brain image, 3(b). The enhanced image using AAIHE

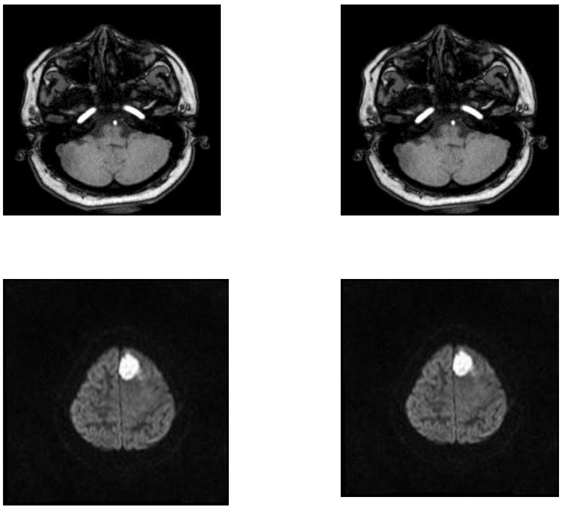

(a) (b)

Fig. 3(a). AAIHE Equalized image, 3(b). FANLMF Filtered image

Algorithm1:

1. Get all inputs: images, amount of fields in rows and rows, histogram containers to use to create variable image function (dynamic range), limit delimation limit (normal 0 to 1)
2. Prior to processing input: Set the exact limit of the clip from the normal value, if necessary, adjust the image before dividing it into the area

3. Process each area context (tile), and be able to produce image of grayscale: the single-zone retrieval of the image, creating the graph of the area using the amount of bins, the histogram snap using the set of the set Create conversion (changes function) for this area
4. Correct image of gray level, in order to collect the final image of AAIHE: retrieved from clusters of four adjacent features of the image processing map area by each tile-over-part artwork, download the application Pixel of Four Map Exercises to the Pixel and Interpolate between Results to Get This Pixel Out! Repeat the whole image.

Next, for pre-processing, Fuzzy Adaptive Non Local Mean Filter (FANLMF) is employed on an enhanced MR brain images for de-noising. This filter processes corrupted images by identifying noise. The pixel process checks whether it is strong or not. That means that if the pixel runs between the maximum and minimum values of the gray level, it is considered to be in pixel, it is still unchanged. If the PPP process takes up the maximum green level, and the minimum is a puzzling pixel running by FANLMF. The Resultant image of above FANLMF is given as an input image to NLMF. This filter provides a superior performance by removing noise while preserving image details. And it allows smoothing image at homogeneous areas without blurring edges. The denoised MR images using MDBUTMF are depicted in Fig. 3.

B. Feature Retrieval

After denoising and contrast enhancement process, the next process is to retrieve the features from the proprocess images. This work introduced one innovative scheme for retrieving deep features from the MR image named Deep Weber Dominant Local Order Based Feature Generator (DWDLOBFG).

Patch Based Deep Local Feature Learning (PBDLFL)

In LBP, All neighbors that have values higher than the value of the center pixel are given value 1 and 0 otherwise. The binary numbers associated with the neighbors are then read sequentially to form a binary bit string. The equivalent of this binary number (usually converted to decimal) may be assigned to the center pixel and it may be used to characterize the local texture. The LBP technique produced the best result even in image rotation process but it does not perform well in image size variation (scaling in size).

To solve this drawback, this work introduces three types of discrete filters before applying LBP directly on to the image for extracting the features in an efficient manner. In order to improve the detection accuracy, the deep discrete transform coefficient LBP features are extracted by using the Convolution Neural Network (CNN).

A CNN consists of one or more convolutional layers, often with a subsampling layer, which are followed by one or more fully connected layers as in a standard neural network. These CNN are used for classification. But in this paper, CNN is used for extracting the deep features from the input satellite image. So in this work, CNN is designed with three convolutional layers, with pooling layers.

Convolution Layer

In a CNN, convolution layers play the role of feature extractor. In this work discrete cosine transform, discrete Fourier transform and discrete wavelet transform encoded LBP features are extracted from the convolution layers. Normally satellite image contains coarse and fine information. Coarse information is good at describing abstract and general characters of buildings while fine information is useful for expressing concrete and detailed characters.

Change detection task needs to extract the fine information from the image to improve the detection accuracy. So this work uses the discrete cosine transform, discrete Fourier transform and discrete wavelet transform encoded LBP techniques to extract the fine features of buildings in the given satellite image.

To extract these features, first, the discrete transform filters (DCT, DFT, DWT) is generated and then apply the convolution operation by using below equation 4.10 to extract the deep features.

$$TI(i,j) = \sum_{m=-1}^{1} \sum_{n=-1}^{1} I(i+m, j+n) \times K(m,n) \quad (4.10)$$

where TI is the convolved image, I is the input image, K is the filter kernel of dimensions k1×k2. The kernel size is 3x3. The discrete transform helps separate the image into parts (or spectral sub-bands) of differing importance. And then LBP is applied on transformed coefficients to encode them to formulate PBDLFL. These the three transform operation is executed on the convolution layer of the CNN.

Pooling Layer

The pooling layer performs downsampling, that is, to reduce the amount of computation time by reducing the extracted features. There are two kinds of pooling layers: max pooling and average pooling. In max pooling, this work takes only the value of the largest pixel among all the pixels in the receptive field of the filter. In the case of average pooling, this work takes the average of all the values in the receptive field. After completing three layers the output of the three pooling layers are combined and come as the output features. These features are called PBDLFL features.

C. Segmentation

After retrieving the feature the next step is to partition the brain image based on these retrieved features using supervised segmentation scheme. Among various supervised segmentation approaches this work only concentrate the machine learning approaches. From the various machine learning approaches this work takes only Self Similarity Multi Level Clustering.

Self Similarity Multi Level Clustering

The SSMLC-based brain segment is divided into two stages: offline and online. The number of images is divided into different categories using label names, such as brain images and non-brain images. Etc. In the training phase, preprocessing, refinement, and classification were performed with the loss function to model the predictions. First, tag the training image. In the previous image processing, resizing was applied to resize the image. Finally, SSMLC is used to automatically classify the brain into the brain. Brain imaging data sets were retrieved from the image network. Image mesh is one of the pre-trained models. If you want to train from the first layer, we need to train the whole layer to the last layer. Therefore, the time consumption is very high. This will affect performance.

To avoid this, a pre-trained model based on brain data was used for ranking steps. In the provided SSMLC, we will only teach the last layer in Python implementation. We do not want to train all layers. Therefore, computational time is low, while high productivity in the scheme of auto-classification of proposed brain tumors. The loss function is calculated using the gradient generation algorithm. The raw pixels of the images were compared to the class estimates using the evaluation function. The quality of a given set is measured by the loss function. It is based on the results obtained with the key labels in the offline data approved. Calculating the loss function is crucial for improving accuracy. If the function loses high when the accuracy is low. Similarly, accuracy is high when the function is low. The slope value is calculated as a loss function to calculate the slope algorithm.

Repeatly evaluate the gradient value to compute the gradient of loss function. Algorithm for SSMLC based segmentation is shown in Algorithm 2. The detected brain regions from the given MR image using v is shown in Fig.6

Algorithm 2

1. Apply convolution filter in first layer
2. The sensitivity of filter is minimized through smoothing the convolution filter (i.e) subsampling
3. Transferring the signal from one layer to another is controlled by an activation layer
4. 4. Tighten up the training period using the Rectified Linear Unit (RELU)
5. Neurons in the flow layer are associated with each neuron in the next layer
6. During a offline process at the end add a loss layer to give feedback to the neural network

IV. EXPERIMENTAL RESULTS

A. DataSet used

Dataset are used in our experiments are collected from the website http://neobrains12.isi.uu.nl/register.php. This site provides both training and testing datasets separately. A total of 4,800 images of the brain were evaluated. The proposed scheme is applied to the image of the brain. During the training phase, a 4,000-millimeter brain tumor was employed, but each had 1000 pieces of brain. Fig. 4 depicts the sample brain tumor images from the database.

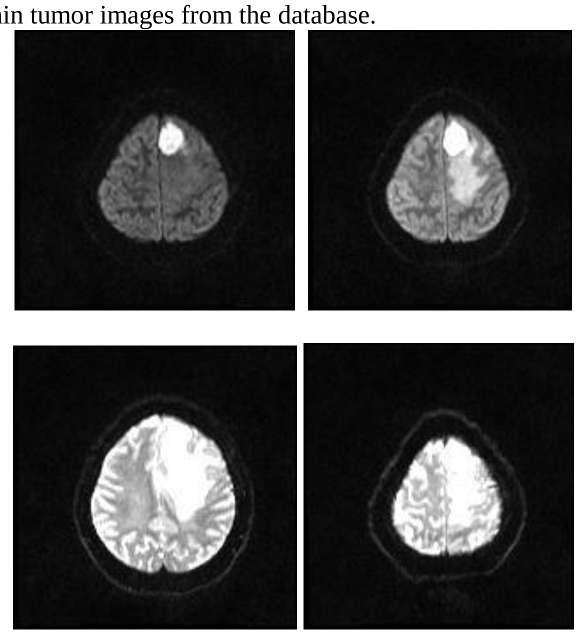

Fig. 4 Experimental Images

B. Performance Metric

The assessment of the supervised machine learning segmentation approaches, this paper employs four metrics namely Dice Similarity Coefficient (DSC), Positive Predictive Value (PPV), Jaccard Index (JI) and Sensitivity (SEN). The DSC [26] metric calculates the overlap among the ground truth and the machine learning segmentation result based on Eq.(4).,

$$DSC = \frac{2TP}{FP+2TP+FN} \quad (4)$$

Where True Negative (TN) signifies the amount of brain tumor pixels accurately predicted. True Positive (TP) signifies the amount of non brain tumor pixels accurately predicted.

False Positive (FP) signifies to the amount of brain tumor pixels wrongly predicted as non brain tumor pixels. False Negative (FN) corresponds to the amount of non brain tumor wrongly predicted as brain tumor pixels. PPV is a calculated of the amount of FP and TP based on Eq.(5),

$$PPV = \frac{TP}{FP+FP} \quad (5)$$

The Jaccard Index is calculated as the amount of the intersection of the brain tumor and non brain tumor pixels separated by the amount of their combination based on Eq.(6),

$$JI = \frac{TP}{TP+FP+FN} \quad (6)$$

At last, Sensitivity metric is calculated to estimate the amount of TP and FN based on Eq.(7),

$$SEN = \frac{TP}{TP+FN} \quad (7)$$

C. Experimental Analysis

Experiment No 1: Analysis of Feature Retrieval Approaches

In this experiment, we will evaluate the contribution of each feature retrieval approaches which are employed in the work. To evaluate the performance of this feature retrieval scheme, the PPV, DSC, JI and SEN measures are employed. It is shown in equation 4,5,6 and 7 correspondingly. Ideally, a excellent feature retrieval scheme is accepted to have a high PPV, DSC, JI and SEN value. Table 1 lists the PPV, DSC, JI and SEN measures of feature retrieval approaches.

Table 1: Analysis of PPV, DSC, JI and SEN of Feature Retrieval Approaches

DataSet				
Feature Descriptor				
Metrics	DSC	PPV	JI	SEN
LBP	83.093	91.993	95.213	94.633
LDP	84.003	93.013	94.383	95.723
LTP	84.523	91.603	95.603	94.203
DERLDP	96.333	94.973	97.633	97.393
PBDLFL	98.765	97.864	98.965	98.993

As observed from Table 1, the PPV, DSC, JI and SEN of the PBDLFL in range 97-98, which is superior than that of the traditional individual feature retrieval method. So the PBDLFL features are best for the brain tumor detection scheme. Fig.8 depicted the PPV, DSC, JI and SEN measures of feature retrieval approaches.

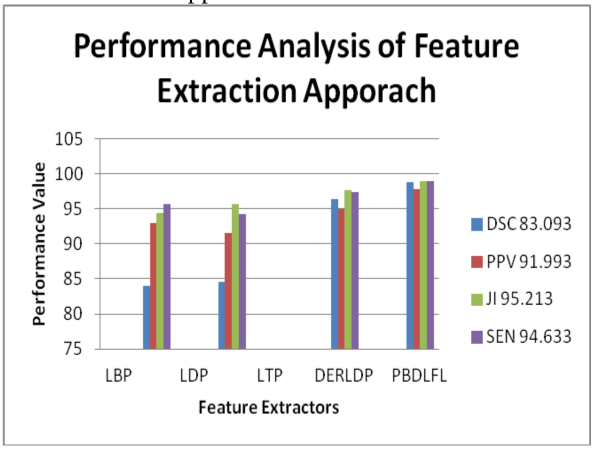

Fig. 5 Analysis of PPV, DSC, JI and SEN of Feature Retrieval Approaches

As observed from Fig.5, the PPV, DSC, JI and SEN of the PBDLFL in range 95-96, which is superior than that of the traditional individual feature retrieval method. So the combined features are best for the brain tumor detection scheme.

Experiment No 2: Analysis of Brain Segmentation Approaches

In this experiment, this work will evaluate the contribution of each brain segmentation approaches which are employed in the work. To assess the efficiency of this brain partition technique, the PPV, DSC, JI and SEN measures are employed. It is shown in equation 4,5,6 and 7 correspondingly. Ideally, a good brain tumor segmentation scheme is expected to have a high PPV, DSC, JI and SEN value. Table 2 lists the PPV, DSC, JI and SEN measures of brain tumor segmentation approaches. As observed from Table 2, the PPV, DSC, JI and SEN of the SSMLC in range 96-97, which is superior than that of the other machine learning brain tumor segmentation scheme. So the SSMLC is best for the brain tumor detection scheme. Fig.6 depicted the PPV, DSC, JI and SEN measures of brain tumor segmentation approaches.

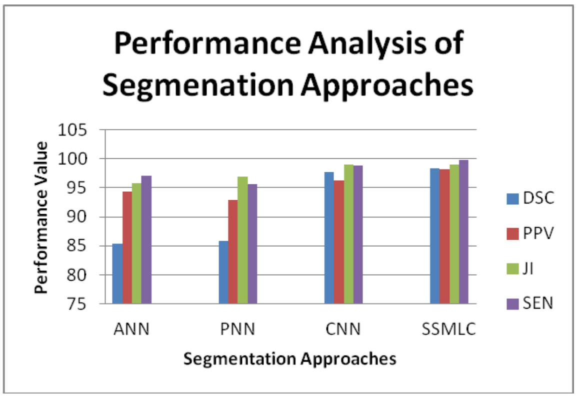

Fig. 6 Analysis of PPV, DSC, JI and SEN of Brain Segmentation Approaches

As observed from Fig.6, the PPV, DSC, JI and SEN of the SSMLC in range 96-98, which is superior than that of the other machine learning brain tumor segmentation scheme. So the SSMLC is best for the brain tumor detection scheme.

Table 2: Analysis of PPV, DSC, JI and SEN for Brain Segmentation Approaches

DataSet				
Machine Learning Segmentation				
Metrics	DSC	PPV	JI	SEN
ANN	85.36	94.37	95.74	97.08
PNN	85.88	92.96	96.96	95.56
CNN	97.69	96.33	98.99	98.75
SSMLC	98.32	98.15	98.92	99.82

Experiment No 3: Analysis of Proposed Feature Retrieval Scheme based Various Kernel Size

In this experiment, we will evaluate the proposed feature retrieval approaches which are employed in the work by varying kernel size. To evalussate the performance of this feature retrieval scheme, the PPV, DSC, JI and SEN measures are employed. It is shown in equation 4,5,6 and 7 correspondingly. Ideally, a excellent feature retrieval scheme is accepted to have a high PPV, DSC, JI and SEN value. Table 1 lists the PPV, DSC, JI and SEN measures of feature retrieval approaches.

Table 1: Analysis of PPV, DSC, JI and SEN of Feature Retrieval Scheme with Various Kernel Size

DataSet				
Kernel Size				
Metrics	DSC	PPV	JI	SEN
3x3	92.174	91.003	93.492	93.004
7x7	93.074	91.903	94.392	93.904
5x5	94.214	93.043	95.532	95.044
9x9	95.234	94.063	96.552	96.064
11x11	97.324	96.153	98.642	98.154

As observed from Table 1, the PPV, DSC, JI and SEN of the 11x11 kernel size in range 97-98, which is superior than that of the other kernel size. So the proposed feature retrieval scheme provides best result in 11x11 kernel size. Fig.7 depicted the PPV, DSC, JI and SEN measures of feature retrieval approaches.

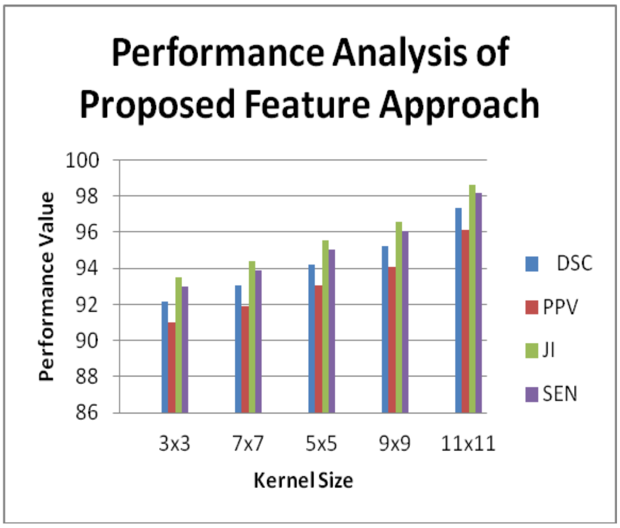

Fig. 7 Analysis of PPV, DSC, JI and SEN of BRATS 2015 for Various Kernel Size

As observed from Fig.7, the PPV, DSC, JI and SEN of the Kernel Size 11x11 in range 97-98, which is superior than that of the other kernel size of the proposed feature retrieval scheme. So the 11x11 kernel size is best for the proposed feature scheme.

V. CONCLUSION

Segmenting the neonatal brain is a complicated task, so errors can lead to more. This paper presented a proposed deep feature retrieval scheme Patch Based Deep Local Feature Learning (PBDLFL) and proposed segmentation method Self Similarity Multi Level Clustering for neonatal brain region segmentation. The process of these approaches is evaluated by PPV, DICE, Sensitivity and Jaccard. This experiment was conducted on the BRATS 2015 database. The article concludes that PBDLFL with SSMLC method provides the best results compared to other approaches. According to DICE and Jaccard data, this article claims that the results of PBDLFL with the SSMLC section are very similar to that part of the truth. To improve SSMLC, this article aims to expand the image of the training as well as to create an effective technique for retrieving features to enhance SSMLC efficiency.

REFERENCES

1. Makropoulos, I.S. Gousias, C. Ledig, P. Aljabar, A. Serag, et al., Automatic whole brain MRI segmentation of the developing neonatal brain, IEEE Trans. Med. Imaging 33 (9) (2014) 1818–1831.
2. Melbourne, M.J. Cardoso, G.S. Kendall, N.J. Robertson, N. Marlow, S. Ourselin, NeoBrainS12 challenge: adaptive neonatal MRI brain segmentation with myelinated white matter class and automated extraction of ventricles I-IV, in: MICCAI Grand Challenge: Neonatal Brain Segmentation (NeoBrainSI2), 2012, pp.16-21.
3. Antonios Makropoulos et al., "A review on automatic fetal and neonatal brain MRI segmentation," NeuroImage, 2017.
4. B.R. Sajja, S. Datta, R. He, M. Mehta, R.K. Gupta, et al., Unified approach for multiple sclerosis lesion segmentation on brain MRI, Ann. Biomed. Eng. 34 (2006) 142–151.
5. Christian Wachinger, Martin Reuter, and Tassilo Klein, "Deepnat: Deep convolutional neural network for segmenting neuroanatomy," NeuroImage, 2017.

6. Dong Nie et al., "Fully convolutional networks for multi-modality isointense infant brain image segmentation," in 13th International Symposium on Biomedical Imaging (ISBI), 2016. IEEE, 2016, pp. 1342–1345.
7. I.S. Gousias, A. Hammers, S.J. Counsell, A.D. Edwards, D. Rueckert, Automatic segmentation of pediatric brain MRIs using a maximum probability pediatric atlas, in: IEEE International Conference on Imaging Systems and Techniques (IST), 2012b, pp. 95–100.
8. I.S. Gousias, A. Hammers, S.J. Counsell, L. Srinivasan, M.A. Rutherford, et al., Magnetic resonance imaging of the newborn brain: automatic segmentation of brain images into 50 anatomical regions, PLoS ONE 8 (4) (2013).
9. I.S. Gousias, A.D. Edwards, M.A. Rutherford, S.J. Counsell, J.V. Hajnal, et al., Magnetic resonance imaging of the newborn brain: manual segmentation of labelled atlases in term-born and preterm infants, NeuroImage 62 (2012) 1499–1509.
10. J. Kittler, M. Hatef, R.P.W. Duin, J. Matas, On combining classifiers, IEEE Trans. Pattern Anal. Mach. Intell. 20 (1998) 226–239.
11. J.F. Mangin, Entropy minimization for automatic correction of intensity nonuniformity, in: IEEE Workshop MMBIA, Hilton Head Island, South Carolina, 2000, pp. 162–169.
12. Jose Dolz et al., "3D fully convolutional networks for subcortical segmentation in MRI: A large-scale study," NeuroImage, 2017.
13. Konstantinos Kamnitsas et al., "Efficient multi-scale 3D CNN with fully connected CRF for accurate brain lesion segmentation," Medical image analysis, vol. 36, pp. 61– 78, 2017.
14. Li Wang et al., "Automatic segmentation of neonatal images using convex optimization and coupled level sets," NeuroImage, vol. 58, no. 3, pp. 805–817, 2011.
15. Li Wang et al., "Segmentation of neonatal brain MR images using patch-driven level sets," NeuroImage, vol. 84, pp. 141–158, 2014.
16. M Jorge Cardoso et al., "AdaPT: an adaptive preterm segmentation algorithm for neonatal brain MRI," NeuroImage, vol. 65, pp. 97–108, 2013.
17. M. Cabezas, A. Oliver, X. Lladó, J. Freixenet, M.B. Cuadra, A review of atlasbased segmentation for magnetic resonance brain images, Comput. Methods Programs Biomed. 104 (2011) e158–e177.
18. M. Modat, G.R. Ridgway, Z.A. Taylor, M. Lehmann, J. Barnes, et al., Fast freeform deformation using graphics processing units, Comput. Methods Programs Biomed. 98 (3) (2010) 278–284.
19. M.J. Cardoso, A. Melbourne, G.S. Kendall, M. Modat, C.F. Hagmann, et al., Adaptive neonatal brain segmentation, MICCAI Lect. Notes Comput. Sci. 6893 (2011) 378–386.
20. M.J. Cardoso, A. Melbourne, G.S. Kendall, M. Modat, N.J. Robertson, et al., AdaPT: an adaptive preterm segmentation algorithm for neonatal brain MRI, NeuroImage 65 (2013) 97–108.
21. Mohammad Havaei, Nicolas Guizard, Nicolas Chapados, and Yoshua Bengio, "Hemis: Hetero-modal image segmentation," in International Conference on Medical Image Computing and Computer-Assisted Intervention. Springer, 2016, pp. 469–477.
22. N.A. Parikh, R.E. Lasky, C.N. Garza, E.B. Mejia, S. Shankaran, et al., Volumetric and anatomical MRI for hypoxic-ischemic encephalopathy: relationship to hypothermia therapy and neurosensory impairments, J. Perinatol. 29 (2009) 143–149.
23. N.A. Parikh, R.E. Lasky, K.A. Kennedy, F.R. Moya, L. Hochhauser, et al., Postnatal dexamethasone therapy and cerebral tissue volumes in extremely low birth weight infants, Pediatrics 119 (2007) 265–272.
24. N.I. Weisenfeld, S.K. Warfield, Automatic segmentation of newborn brain MRI, NeuroImage 47 (2) (2009) 564–572.
25. Pim Moeskops et al., "Automatic segmentation of MR brain images with a convolutional neural network," IEEE Transactions on Medical Imaging, vol. 35, no. 5, pp. 1252–1261, 2016.
26. Tobias Fechter et al., "Esophagus segmentation in CT via 3D fully convolutional neural network and random walk," Medical Physics, 2017.
27. V.S. Egekher, M.J.N.L. Benders, M.A. Viergever, I. Isĝum, Automatic neonatal brain tissue segmentation with MRI, in: Proc. SPIE 8669, Medical Imaging, 2013, Image Processing, 2013.
28. W. Zhang et al., "Deep convolutional neural networks for multi-modality isointense infant brain image segmentation," NeuroImage, vol. 108, pp. 214–224, 2015.
29. X. Yu, Y. Zhang, R.E. Lasky, S. Datta, N.A. Parikh, et al., Comprehensive brain MRI segmentation in high risk preterm newborns, PLoS ONE 5 (11) (2010).
30. Z. Song, Statistical Tissue Segmentation of Neonatal Brain MR Images, Dept. of Bioengineering, Univ. of Pennsylvania, 2008, Ph.D. Dissertation.

AUTHORS PROFILE

I am **Puja Shashi**, currently doing Phd research in the domain of computer application under the main title Image processing from Jain University. I am having ten years of teaching and administrative experience in various reputed institution. I am working under Dr. Suchithra Nair, Associate professor, HOD MSc IT, Jain University as my mentor and guide. This Paper is a part of my research work regarding automated segmentation of neonatal brain.

R.Suchithra is the director of MCA department in Jain Deemed to be University,Bangalore . She has 16 years of experience in teaching and research .She has published more than 24 papers in reputed journals and her area of specialization is on cloud computing , machine learning and data science . She is guiding research scholars in the PhD programme

.

Retrieval Number: D9579118419/2019©BEIESP
DOI:10.35940/ijrte.D9579.118419
Journal Website: www.ijrte.org

Published By:
Blue Eyes Intelligence Engineering
& Sciences Publication